Journal of Innovative Optical Health Sciences
Vol. 4, No. 1 (2011) 67–72

DOI: 10.1142/S1793545811001216

CHARACTERIZATION OF VITILIGO BY *IN VIVO* SCATTERING COEFFICIENT OF HUMAN SKIN

WANRONG GAO*, PENG LEE and XIANLING ZHANG
Department of Optical Engineering
Nanjing University of Science and Technology
200 Xiao Ling Wei, Nanjing
Jiangsu 210094, China
**gaowangrong@yahoo.com*

Scattering coefficients of human skin *in vivo* with and without vitiligo were measured with optical coherence tomography (OCT). The experimental results show that there exist significant difference between the scattering coefficient of the epidermis of *in vivo* human skin with and without vitiligo disease. The results may be helpful for quantitatively diagnosing or evaluating the treatment of the disease.

Keywords: Scattering coefficient; human skin; vitiligo; optical coherence tomography.

1. Introduction

Since the first optical coherence tomography of the human retina and optic disk *in vitro* were obtained by optical coherence tomography (OCT),[1] high-resolution cross-sectional images of various types of tissues have been generated successfully with this technique. Several excellent review articles about the applications of OCT have been published.[2–10] Several theoretical models have also been proposed to evaluate the imaging performance of OCT systems such as its depth resolution and signal-to-noise ratio, or to find out what information about the microstructures of tissues can be measured by OCT systems.[11–17] Because of the strong scattering, the great challenge for theoretical analysis is how to describe the scattering process for probing light beam propagating through the tissue. The simplest approximation is the single scattering approximation, in which the contribution to the measured detector signal is assumed to be arising from the light only and there is backscattering from tissue.[11,12] To consider the effect of the multiple scattered light, the extended Fresnel principle has been employed.[18] Because the OCT signal is depth-resolved localized reflectivity or backscattering characteristic of tissue, it is possible to use OCT to measure the backscattering coefficients.[11] Realizing that OCT has the capability of accurately measuring the axial optical path length in the sample arm, OCT has been employed to measure the average refractive index of *in vitro* tissues.[19–23] Due to the tissue degradation and dehydration, the refractive index of *in vivo* tissue may be different from that of *in vitro* tissue. Tearney *et al.*[19] then measured the refractive index of *in vivo* tissue placed in the sample arm of OCT system by tracking the focal position of the sample objective as the sample was scanned through the focus. Because the scattering of light in tissue arises from the spatial variations in refractive index, Schmitt and Kumar[24] investigated the characteristics of the spatial variations in the index of refraction of a variety of tissues.[24] More recently, by using calibrated samples in the fixed

*Corresponding author.

focus geometry, the validity of the single-scattering and multiple-scattering models for both the highly-scattering and weakly-scattering media have been investigated.[25] The results show that with a proper correction for the confocal properties of the sample arm, both models are appropriate for the extraction of scattering coefficients of the weakly scattering media. For the highly-scattering media, the multiple-scattering model is more accurate.

In this work, we will use the method developed in Ref. 25 to obtain the averaged scattering coefficients of human skin *in vivo* with and without vitiligo disease. The results may be helpful for quantitatively diagnosing or evaluating the treatment method.

2. Theory

As pointed out above, for weak scattering medium the light signal backscattered from within the sample can be described by the single scattering approximation. On the other hand, for strong scattering medium such as human skin, the multiple-scattering model based on the extended Fresnel principle may be employed.[16,23] According to this model, the OCT signal can be expressed as[18,25]:

$$i(z) \propto \left[\exp(-2\mu_s z) + \frac{2\exp(-\mu_s z)[1-\exp(-\mu_s z)]}{1+\omega_S^2/\omega_H^2} + [1-\exp(-\mu_s z)]^2 \frac{\omega_H^2}{\omega_S^2}\right]^{1/2}. \quad (1)$$

The first term in Eq. (1) represents the single-backscatter contribution; the third term represents the contribution from multiple-scattering events, while the second term is the cross-term. The quantities ω_H and ω_S are the $1/e$ irradiance radius at the probing depth in the absence and presence of scattering, respectively, given by

$$\omega_H^2 = \omega_0^2\left(A - \frac{B}{f}\right)^2 + \left(\frac{B}{k\omega_0}\right)^2, \quad (2)$$

$$\omega_S^2 = \omega_0^2\left(A - \frac{B}{f}\right)^2 + \left(\frac{B}{k\omega_0}\right)^2 + \left(\frac{2B}{k\rho_0(z)}\right)^2, \quad (3)$$

where A and B are elements from the ABCD ray-matrix for light propagation from the lens plane to the probing depth in the sample. The quantity ω_0 represents the $1/e$ irradiance radius of the input sample beam at the objective lens plane, k is the wave number, f is the focal length of the lens, and $\rho_0(z)$ is the lateral coherence length. $\rho_0(z)$ is given by[11]

$$\rho_0(z) = \sqrt{\frac{3}{\mu_s z}}\frac{\lambda_0}{\pi\theta_{\text{rms}}}\left(\frac{nB}{z}\right)^2, \quad (4)$$

where n is the mean index of refraction of the sample, and θ_{rms} represents the root-mean-square scattering angle,

$$\theta_{\text{rms}} \approx \sqrt{2(1-g)}, \quad (5)$$

where g is the anisotropy factor. Equation (1) is appropriate for the dynamic focusing geometry, and the confocal property of the sample arm, i.e., the position of the focus in the sample and the depth of focus were not considered. For the fixed focusing arrangement, the divergence of the light beam generates an additional loss of signal and makes the extracted μ_s higher than the expected values. For OCT system to consider the effect of confocal properties of the sample arm optics, an axial confocal PSF can be employed, which can be expressed as[26,27]

$$h(z) = \left(\left(\frac{z-z_f}{z_R}\right)^2 + 1\right)^{-1}, \quad (6)$$

where the position of the focal plane $z_f = 0$, and z_R is the "apparent" Rayleigh length used to characterize the PSF. In this study z_R was fixed at 99 μm during the processes of scattering coefficient extraction.

3. Results and Discussion

Vitiligo is a commonly encountered dermatosis. In China, about 0.1% to 2% of the normal people may suffer from this disease, i.e., nearly 1 million to 20 million people may catch vitiligo. The fact that vitiligo usually occurs on the exposed parts of the human body such as the face, feet, and hands, brings people much stress because it affects the appearance of the image of people. Furthermore, vitiligo is very difficult to cure. At present there is no specific remedy. The basic pathological change of vitiligo is that the melanocyte of skin tissue partly or totally loses its function, leading to the shortage of the melanocytes in epidermis of the skin. Hence, the basic purpose of treatment is to help the melanocyte to recover the capability of melanocyte or to

stimulate the development of the melanocyte to generate more melanins. The major function of melanins in human skin is solar photoprotection, provided through optical absorption and scattering by epidermal melanosomes.[28] Because the refractive index of melanin is much higher than other elements of tissue and cells (1.7),[28–30] it is expected that the scattering coefficient and refractive index of skin with vitiligo disease may change.

The measurements of the scattering coefficients of the skin with and without vitiligo were performed with the OCT system developed in our lab. The detailed description of the system can be found in Ref. 25. Briefly, a light beam from a superluminescent diode (SLD) (central wavelength $\lambda_0 = 834\,\text{nm}$, output power $\sim 2\,\text{mW}$, coherence length 14.5 μm in free space) illuminates a single-mode fiber-optic Michelson interferometer along with an aiming beam of a cw laser diode with the wavelength of 658 nm. The light was split into the sample and reference arms by a 50×50 beam splitter. A mirror on a translation stage was moved at a constant velocity $V = 11\,\text{mm/s}$ over the measurement range to vary the optical path length in the reference arm and simultaneously modulate the frequency of the interference signal at Doppler-shift frequency $f_0 = 2V/\lambda_0 = 26.4$ kHz, together with bandwidth $B = 2V\Delta\lambda/\lambda_0^2 = 0.67$ kHz.

The magnitude of the interference signal was measured by a photodiode, and demodulated on its Doppler-shift frequency. And then, the root-mean-squared (rms) power of the resultant signal was digitized and stored in a computer. B-scan was performed by moving the sample arm beam with respect to the fixed sample. In each B-scan, 200 consecutive in-depth scans were acquired. The 2D images were reconstructed by LabVIEW. The sensitivity of −90 dB was obtained by the OCT system. In this system, the fixed focus geometry is employed, i.e., the focal plane of the sample beam is fixed on the top of the surface of the sample in all experiments. For the geometry, $A = 1$ and $B = f + z/n$. The $1/e$ irradiance radius of the input sample beam at the objective lens plane is determined by the fiber collimator, and $\omega_0 = 1.07\,\text{mm}$, the focal length of the objective lens $f = 18\,\text{mm}$.

Figure 1 shows the image of skin of the back of the right hand of a volunteer with vitiligo disease obtained with a CCD camera. The positions and the areas of the skin with vitiligo are clearly shown. In Figs. 2 and 3 *in vivo* OCT images of normal human skin of the left forearm of a volunteer and *in vivo* OCT image of human skin of the right forearm of a volunteer with vitiligo disease are displayed. It can be seen from the images that both the epidermis and the upper dermis can be identified.

Fig. 1. Image of skin of the back of the right hand of a volunteer with vitiligo disease obtained with a CCD camera.

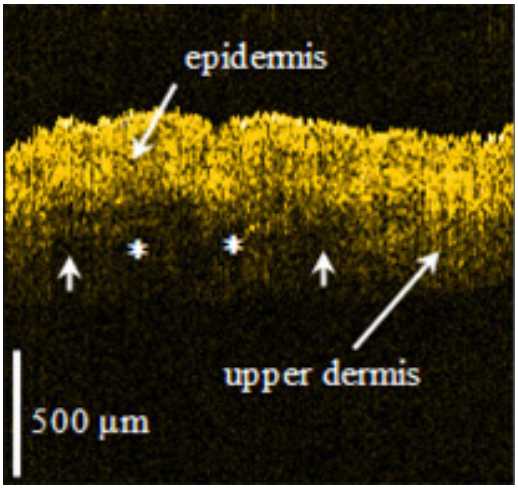

Fig. 2. *In vivo* OCT image of normal human skin of the left forearm of a volunteer without vitiligo disease.

Figure 4 shows curve of the averaged OCT in-depth signal of normal human skin of the left forearm of a volunteer without vitiligo disease and the fitted curve for the epidermis by using EHF model. Figure 5 displays the curve of the averaged OCT in-depth signal of the right forearm of a volunteer with vitiligo disease and the fitted curve for the epidermis by using EHF model. The scattering coefficients μ_s were extracted by fitting the model to the signal corresponding to the epidermis in the OCT image. To improve the accuracy of the scattering

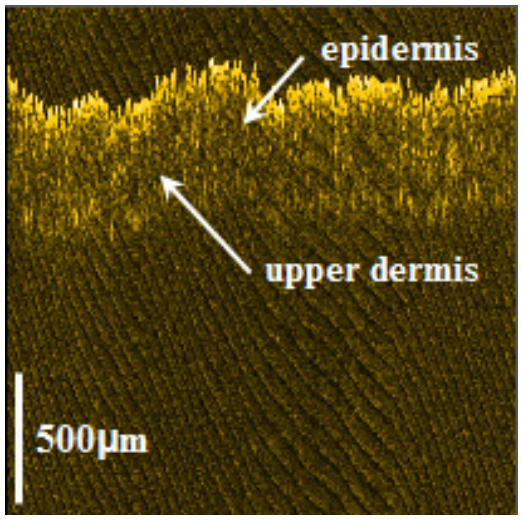

Fig. 3. *In vivo* OCT image of human skin of the right forearm of a volunteer with vitiligo disease.

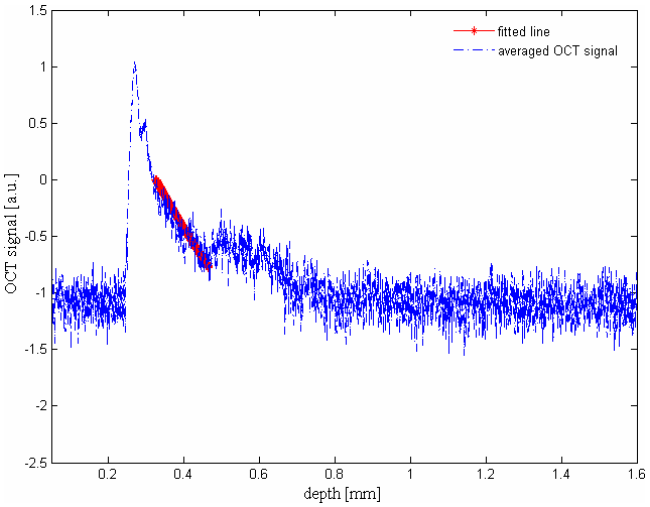

Fig. 4. Curve of the averaged OCT in-depth signal of normal human skin of the left forearm of a volunteer without vitiligo disease and the fitted curve for the epidermis using EHF model.

coefficient μ_s, the average of the signals obtained from different sites of the sample (spatial averaging) were calculated to reduce the effects of the speckle.[31,32] To remove the effect of the rough skin surface on the accuracy of the estimation of the scattering coefficient, the 200 in-depth scans in each image were first divided into 10 groups, OCT signals were then calculated by averaging over 20 in-depth scans in extraction of scattering coefficients μ_s (mm^{-1}). Finally, the average scattering coefficient μ_s was obtained by calculating the average of the 10 values of scattering coefficients μ_s. It was

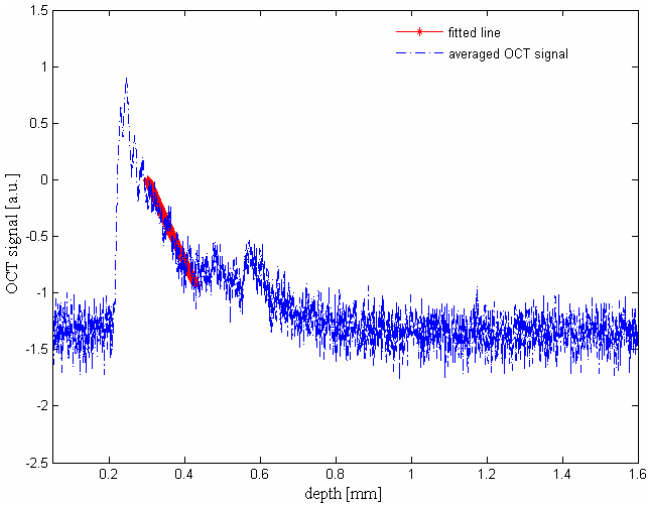

Fig. 5. Curve of the averaged OCT in-depth signal of the right forearm of a volunteer with vitiligo disease and the fitted curve for the epidermis using EHF model.

found that the average scattering coefficient of the epidermis of the forearm with vitiligo disease is $(4.56 \pm 0.31)\ \mathrm{mm}^{-1}$, and the corresponding value for normal epidermis of the forearm is $(5.59 \pm 0.50)\ \mathrm{mm}^{-1}$. With the same method, the scattering coefficients of the back skin of the hands with vitiligo disease and without vitiligo disease are $(4.79 \pm 0.32)\ \mathrm{mm}^{-1}$ and $(5.88 \pm 0.34)\ \mathrm{mm}^{-1}$, respectively. These changes in scattering coefficients may result from the decrease of melanin in skin tissue. As mentioned above, the pathological change of vitiligo is that the melanocyte of skin tissue partly or totally loses its function, leading to the shortage of the melanocytes in the epidermis of the skin. As a consequence, the generation of melanin decreases. Because melanin has higher refractive index than other cell components,[30] the spatial distribution of the refractive index in skin tissue with vitiligo varies, resulting in the change in scattering coefficients.

In conclusion, scattering coefficients of human skin *in vivo* with and without vitiligo were obtained by fitting the model to the signal measured with OCT. The experimental results show that there exist significant changes in the scattering coefficient of the epidermis of *in vivo* human skin with vitiligo disease. Hence, quantitative measurement of the scattering coefficient of *in vivo* human skin with vitiligo disease may be helpful for quantitatively diagnosing or evaluating the treatment of the skin disease.

Acknowledgments

This research was supported by the National Natural Science Foundation of China (60978069), the Provincial Natural Science Foundation of Jiangsu Province (BK2008412), the Research Foundation for the Doctoral Program of Higher Education of China (200802880013), and the 333 Talent Project Foundation of Jiangsu Province.

References

1. D. Huang, E. A. Swanson, C. P. Lin, J. S. Schuman, W. G. Stinson, W. Chang, M. R. Hee, T. Flotte, K. Gregory, C. A. Puliafito, J. G. Fujimoto, "Optical coherence tomography," *Science* **254**, 1178−1181 (1991).
2. J. G. Fujimoto, C. Pitris, S. A. Boppart, M. E. Brezinski, "Optical coherence tomography: An emerging technology for biomedical imaging and optical biopsy," *Neoplasia* **2**, 9−25 (2000).
3. J. G. Fujimoto, "Optical coherence tomography for ultrahigh resolution *in vivo* imaging," *Nature Biotechnol.* **21**, 1361−1367 (2003).
4. A. F. Low, G. J. Tearney, B. E. Bouma, I. K. Jang, "Technology insight: Optical coherence tomography — Current status and future development," *Nature Clin. Practice* **3**(3), 154−162 (2006).
5. M. E. Brezinski, "Applications of optical coherence tomography to cardiac and musculoskeletal diseases: Bench to bedside?," *J. Biomed. Opt.* **12**(5), 051705-1-12 (2007).
6. A. M. Zysk, F. T. Nguryen, A. L. Oldenberg, D. L. Marks, S. A. Boppart, "Optical coherence tomography: A review of clinical development from bench to bedside," *J. Biomed. Opt.* **12**(5), 051403-1-21 (2007).
7. A. Tanaka, G. J. Tearney, B. E. Bouma, "Challenges on the frontier of intracoronary imaging: Atherosclerotic plaque macrophage measurement by optical coherence tomography," *J. Biomed. Opt.* **15**(1), 011104-1-8 (2010).
8. A. F. Fercher, C. K. Hitzenberger, "Optical coherence tomography," in *Progress in Optics*, Vol. 44 (Elsevier, Amsterdam, 2002), Ch. 4, pp. 215−302.
9. Wanrong Gao, "Spectral changes of the light produced by scattering from tissue," *Opt. Lett.* **35**(6), 862−864 (2010).
10. Wanrong Gao, "Square law between Fourier spatial frequency of correlation function of scattering potential of tissue and spectrum of scattered light in the far zone," *J. Biomed. Opt.* **15**(3), 030502 (2010).
11. J. M. Schmitt, A. Knüttel, R. F. Bonner, "Measurement of optical properties of biological tissues by low-coherence reflectometry," *Appl. Opt.* **32**, 6032−6042 (1993).
12. J. A. Izatt, M. R. Hee, G. M. Owen, E. A. Swanson, J. G. Fujimoto, "Optical coherence microscopy in scattering media," *Opt. Lett.* **19**(8), 590−592 (1994).
13. Y. Pan, R. Birngruber, J. Rosperich, R. Engelhardt, "Low-coherence tomography in turbid tissue: Theoretical analysis," *Appl. Opt.* **34**, 6564−6574 (1995).
14. A. F. Fercher, "Optical coherence tomography," *J. Biomed. Opt.* **1**(2), 157−173 (1996).
15. A. G. Podoleanu, D. A. Jackson, "Noise analysis of a combined optical coherence tomography and a confocal scanning ophthalmoscope," *Appl. Opt.* **38**(10), 2116−2127 (1999).
16. J. F. de Boer, B. Cense, B. H. Park, M. C. Pierce, G. J. Tearney, B. E. Bouma, "Improved signal-to-noise ratio in spectral-domain compared with time-domain optical coherence tomography," *Opt. Lett.* **28**(21), 2067−2069 (2003).
17. M. A. Choma, M. V. Sarunic, C. Yang, J. A. Izatt, "Sensitivity advantage of swept source and Fourier domain optical coherence tomography," *Opt. Express.* **11**(18), 2183−2189 (2003).
18. L. Thrane, H. T. Yura, P. E. Andersen, "Analysis of optical coherence tomography systems based on the extended Huygens−Fresnel principle," *J. Opt. Soc. Am. A* **17**, 484−490 (2000).
19. G. J. Tearney, M. E. Brezinski, J. F. Southern, B. E. Bouma, M. R. Hee, J. G. Fujimoto, "Determination of the refractive index of highly scattering human tissue by optical coherence tomography," *Opt. Lett.* **20**, 2258−2260 (1995).
20. A. Knüttel and M. Boehlau-Godau, "Spatially confined and temporally resolved refractive index and scattering evaluation in human skin performed with optical coherence tomography," *J. Biomed. Opt.* **5**, 83−92 (2000).
21. D. Levitz, L. Thrane, M. Frosz, P. Andersen, C. Andersen, S. Andersson-Engels, J. Valanciunaite, J. Swartling, P. Hansen, "Determination of optical scattering properties of highly-scattering media in optical coherence tomography images," *Opt. Express* **12**, 249−259 (2004).
22. F. J. van der Meer, D. J. Faber, D. M. Baraznji Sassoon, M. C. Aalders, G. Pasterkamp, T. G. van Leeuwen, "Localized measurement of optical attenuation coefficients of atherosclerotic plaque constituents by quantitative optical coherence tomography," *IEEE Trans. Med. Imaging* **24**, 1369−1376 (2005).
23. C. Xu, J. M. Schmitt, S. G. Carlier, R. Virmani, "Characterization of atherosclerosis plaques by measuring both backscattering and attenuation

coefficients in optical coherence tomography," *J. Biomed. Opt.* **13**, 034003 (2008).
24. J. M. Schmitt and G. Kumar, "Turbulent nature of refractive-index variations in biological tissue," *Opt. Lett.* **21**, 1310 (1996).
25. P. Lee, W. Gao, X. Zhang, "Performance of single-scattering vs. multiple-scattering model in the determination of optical properties of biological tissue with optical coherence tomography," *Appl. Opt.*, accepted and in press.
26. D. J. Faber, F. J. van der Meer, M. C. G. Aalders, T. G. van Leeuwen, "Quantitative measurement of attenuation coefficients of weakly scattering media using optical coherence tomography," *Opt. Express* **12**, 4353−4365 (2004).
27. T. G. van Leeuwen, D. J. Faber, M. C. Aalders, "Measurement of the axial point spread function in scattering media using single-mode fiber-based optical coherence tomography," *IEEE J. Sel. Top. Quantum Electron.* **9**, 227−233 (2003).
28. I. A. Vitkin, J. Woolsey, B. C. Wilson, R. R. Anderson, "Optical and thermal characterization of natural (sepia officinalis) melanin," *Photochem. Photobiol.* **59**, 455−462 (1994).
29. J. M. Schmitt and G. Kumar, "Optical scattering properties of soft tissue: A discrete particle model," *Appl. Opt.* **37**(13), 2788−2797 (1998).
30. A. Dunn and R. Richards-Kortum, "Three-dimensional computation of light scattering from cells," *IEEE J. Sel. Top. Quantum Electron.* **2**, 898−905 (1996).
31. J. M. Schmitt, S. H. Xiang, K. M. Yung, "Speckle in optical coherence tomography," *J. Biomed. Opt.* **4**, 95−105 (1999).
32. A. I. Kholodnykh, I. Y. Petrova, K. V. Larin, M. Motamedi, R. O. Esenaliev, "Precision of measurement of tissue optical properties with optical coherence tomography," *Appl. Opt.* **42**, 3027−3037 (2003).